



**HAL**  
open science

## Electromagnetic Study of High Power Density: PMSM for Automotive Application

M. Hebri, A. Rebhaoui, Grégory Bauw, Jean-Philippe Lecoïnte, S. Duchesne,  
V. Mallard, G. Zito, A. Abdelli, A. Maier

► **To cite this version:**

M. Hebri, A. Rebhaoui, Grégory Bauw, Jean-Philippe Lecoïnte, S. Duchesne, et al.. Electromagnetic Study of High Power Density: PMSM for Automotive Application. 2022 International Conference on Electrical Machines (ICEM), Sep 2022, Valencia, Spain. pp.28-34, 10.1109/ICEM51905.2022.9910916 . hal-04130930

**HAL Id: hal-04130930**

**<https://hal.science/hal-04130930>**

Submitted on 16 Jun 2023

**HAL** is a multi-disciplinary open access archive for the deposit and dissemination of scientific research documents, whether they are published or not. The documents may come from teaching and research institutions in France or abroad, or from public or private research centers.

L'archive ouverte pluridisciplinaire **HAL**, est destinée au dépôt et à la diffusion de documents scientifiques de niveau recherche, publiés ou non, émanant des établissements d'enseignement et de recherche français ou étrangers, des laboratoires publics ou privés.

# Electromagnetic Study of High Power Density PMSM for Automotive Application

M. A. Hebri, A. Rebhaoui, G. Bauw, J-Ph. Lecoite, S. Duchesne, V. Mallard, G. Zito, A. Abdelli, and A. Maier

**Abstract** -- This paper presents an analytical design method to improve the power density of an interior permanent magnet synchronous machine (PMSM) with multi-variable and multi-objective optimization based on a genetic algorithm (NSGA2). A 12-slot/8-pole topology with fractional-slot concentrated windings (FSCW) has been chosen. Several designs with different mechanical power, rotational speed, and voltage are carried out. As a key result, the increase of the power density of PMSMs is achieved mainly with the increase of the mechanical power, the rotational speed and the current density.

**Index Terms**—Current density, design, efficiency, FSCW, genetic algorithm, NSGA2, optimization, PMSM.

## I. INTRODUCTION

THE transport sector is a source of pollution and greenhouse gas production. Several cities have taken initiatives to promote the use of clean vehicles with a low level of harmful emissions. The electric propulsion offers a solution with no emissions and a good efficiency, with the opportunity to be powered by an electric energy that is becoming more and more renewable.

For this reason, researchers focus their attention on electrical motors. In [1] and [2], the authors proposed respectively a compact and low-cost axial flux permanent magnet machine and a high-speed radial flux permanent magnet motor for automotive application. A switched reluctance motor (SRM) and an induction motor (IM) have been also designed and analyzed in [3] and [4] respectively, for automotive applications. Such an electric machine for traction applications requires basically high torque and power densities, a high starting torque, a wide speed range, a high efficiency for all operating points and over a wide speed and torque ranges, high reliability, robustness and, finally, an acceptable cost [5]. Permanent magnets are commonly used in synchronous machines (PMSM) [5-6]. They have a higher power density, a better efficiency and a more compact size compared to the IM and SRM. PMSM is therefore a good candidate for the expected application.

M.A. Hebri, A. Rebhaoui, G. Bauw, J-Ph. Lecoite, S. Duchesne, are with Univ. Artois, UR 4025, Laboratoire Systèmes Electrotechniques et Environnement (LSEE), Béthune, F-62400, France (e-mail: [mamine.hebri@univ-artois.fr](mailto:mamine.hebri@univ-artois.fr), [rebhaouiabderrahmane@gmail.com](mailto:rebhaouiabderrahmane@gmail.com), [gregory.bauw@univ-artois.fr](mailto:gregory.bauw@univ-artois.fr), [jphilippe.lecoite@univ-artois.fr](mailto:jphilippe.lecoite@univ-artois.fr), [stephane.duchesne@univ-artois.fr](mailto:stephane.duchesne@univ-artois.fr)).

V. Mallard is with CRITT M2A, 62700 Bruay-la-Buissière, France (e-mail: [vmallard@crittm2a.com](mailto:vmallard@crittm2a.com)).

G. Zito and A. Abdelli are with IFP Energies Nouvelles, Rueil-Malmaison, 92852, France. (e-mail: [gianluca.zito@ifpen.fr](mailto:gianluca.zito@ifpen.fr), [abdenour.abdelli@ifpen.fr](mailto:abdenour.abdelli@ifpen.fr)).

A. Maier is with EREM, 60130 Wavignies, France (e-mail: [adrien.maier@erem.fr](mailto:adrien.maier@erem.fr)).

To increase the power density in the PMSM, several solutions are investigated in the literature. In [7], the authors proposed to reduce the mass of copper and steel sheets by increasing the current density. The use of high-performance rare-earth magnets to increase the energy density has been reported in [8]. However, the environmental impact and the high cost are the major drawbacks of the previous solution. In order to improve the power density, several solutions exist as the use of an innovative magnetic steels such as grain-oriented steel sheets [9]. The slot/pole combination can be optimized to modify the winding factor and new type of winding, called fractional-slot concentrated windings (FSCW) are developed [10] to maximize the winding factor. In [11] and [12], the authors proposed new methodologies for optimal design of FSCW to increase the winding factor and, therefore, the power density.

The aim of this paper is to improve the power density and the efficiency by varying several parameters as the current density, the voltage, the mechanical power, and the rotational speed, by considering their maximum value permitted by the thermal or mechanical possibilities. This study is based on an analytical calculation coupled with a multi-objective optimization (Non-dominated Sorting Genetic Algorithm: NSGA2). In the first part, the authors present the electromagnetic design approach of a PMSM as well as the basic sizing equations: torque and back-EMF taking into account the mechanical and thermal limits defined in the literature. The aimed application context concerns electric sports vehicles. In the same part, the authors present the calculation method of the efficiency and the power density. In the second part of the study, a brief presentation of the multi-objective optimization "NSGA2" method is shown as well as the optimization parameters and their range of variation, the optimization constraints and the NSGA2 optimization tool parameters. In the third part, the results of the PMSM analytical design and multi-variable / multi-objective optimization (efficiency, power density) are shown. Also the impact of the different parameters (current density, rotation speed, voltage, and mechanical power) on the efficiency and the power density is presented. In the last part, a PMSM structure is chosen following the analytical design and optimization and it is validated with 2D-FEM analysis. The efficiency map of the structure is presented on the torque/speed plane.

## II. ELECTROMAGNETIC DESIGN OF THE MACHINE

The initial design of electrical machines is based on analytical formulas that aim to determine a first geometry of the machine. It has to be validated by FEM to confirm the

magnetic flux densities in the different parts of the machine (teeth, yoke, air gap) and the back-EMF.

### A. Specifications

The targeted application context concerns the motorization of electric motorsport vehicles. The expected rated power-to-weight ratio of the proposed machine is 8kW/kg, considering only the active parts. This operating point is defined in Table I.

TABLE I  
SPECIFICATIONS

Mechanical power	115 kW
Rotational speed	10 000 rpm
Maximum DC voltage	900 V

### B. Choice of the Motor Topology

In this study, a three-phase interior permanent magnet synchronous machine (IPMSM) has been chosen. IPMSMs are known for their compactness due to the high energy density produced by the magnets. The mechanical strength of this type of rotor allows very high speeds to be reached at high power levels. In addition, the magnets are protected from the demagnetizing stator field. FSCW features shorter end windings, thus reducing the Joule effect losses and allows to design more compact machines, which makes FSCW a suitable winding topology for our application. A 12-slot/8-pole topology is chosen as a test case; the geometry and the notations are shown in Fig. 1.

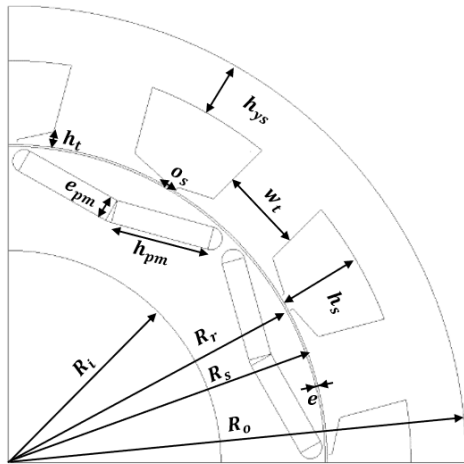


Fig. 1. Representation of the selected geometry.

### C. Electromagnetic design

The method used in this paper starts by considering [13] the torque  $T$  on the rotor as:

$$T = 2 \sigma_{tan} V_r \quad (1)$$

where  $\sigma_{tan}$  is the tangential stress exerted on the rotor surface and  $V_r$  is the rotor volume. The tangential stress can be calculated as a function of the linear current density  $A$  (RMS value) and the peak value  $\hat{B}_\delta$  of the flux density  $B_\delta$  in the air gap:

$$\sigma_{tan} = \frac{A \hat{B}_\delta}{\sqrt{2}} \quad (2)$$

Then, the RMS value of the induced voltage  $E$  is given by:

$$E = \frac{\pi R_r}{\sqrt{2}} \omega_r N k_w L \alpha_i \hat{B}_\delta \quad (3)$$

where  $R_r$  is the rotor radius,  $L$  is rotor length,  $\omega_r$  is the angular velocity,  $k_w$  is the winding factor fundamental,  $N$  is number of turns per phase, and the product  $\alpha_i \hat{B}_\delta$  represents the average value of the air-gap flux density under one pole.

The flux density in the airgap can be approximated by:

$$\hat{B}_\delta = \frac{2 p h_{pm} e_{pm}}{\pi e_{pm} R_r + 2 p h_{pm} e} B_r \quad (4)$$

where  $B_r$  is a remanent flux density.

### D. Design approach

The combination of the equations leads to an expression giving the variation of the volume of the rotor as a function of several electrical parameters. It gives the way to follow to reduce the volume of the rotor and, thus, to increase the power density. If  $m$  is the number of phases and  $I$  is the stator phase current, the apparent power  $S$  is:

$$S = m E I \quad (5)$$

The current can be written:

$$I \approx \frac{A \pi R_r}{N m} \quad (6)$$

By replacing the expression (3) and (5) in (4), we find:

$$D_r^2 L = \frac{2 \sqrt{2} S p}{k_w \hat{B}_\delta A \alpha_i \pi^3 f} \quad (7)$$

where  $f$  is the frequency.

The quantity  $D_r^2 L$  translates the volume of the rotor of the machine. It expresses well the fact that the volume of the machine is, at a given power, inversely proportional to:

- The rotational speed,
- The flux density in the air gap,
- The linear current density.

Thus, if the speed is defined by the specifications or by the peripheral rotor speeds of the rotor on the one hand, and if, on the other hand, the flux density is limited, even with the best materials, to about 1.1 T in the air gap, only the linear load remains to reduce the volume. Its increase requires either the implementation of effective cooling solutions or the use of materials able to withstand the higher temperatures at the core of the machine. This problem is even more aggravated by the difficulty of evacuating the calories generated by the reduction of the volume.

### E. Efficiency analysis of PMSM

The losses of PMSM mainly include four parts: losses in iron, magnets, copper, and mechanical losses. In this analytical design, the magnet losses and mechanical losses are not considered.

Iron losses arise from the establishment of magnetic flux in the laminations made of electrical steel. The iron losses  $P_{iron}$  can be estimated by different models. Bertotti's model is

applied; it decomposed the iron losses into three parts: the hysteresis losses  $P_{hys}$ , the eddy current losses  $P_{eddy}$  and the excess losses  $P_{ex}$ .

$$P_{iron} = (P_{hys} + P_{eddy} + P_{ex}) V \quad (8)$$

Considering only the first harmonic, the losses per volume unity are given by:

$$\begin{cases} P_{hys} = k_{hys} f B_m^2 \\ P_{eddy} = k_{eddy} (f B_m)^2 \\ P_{ex} = k_{ex} f B_m^{1.5} \end{cases} \quad (9)$$

where  $B_m$  is the value of the flux density in the sheet.  $k_{hys}$ ,  $k_{eddy}$  and  $k_{ex}$  are hysteresis loss factor, eddy-current loss factor and excessive loss factor, respectively.

The Joule losses in the winding of AC machines are due to the resistance of the conductors and the currents induced in them. These induced currents are the direct consequence of the variation of the field generated by the rotation of the magnets, by the conductors in their proximity (proximity effect) and by the time-varying current which passes through the conductor itself (skin effect). To make the design easier, only losses due to resistance are considered. Representation of an end-winding is presented in Fig.2.

The copper loss in the stator winding can be expressed as:

$$P_{Joule} = 3 R I^2 \quad (10)$$

The total resistance  $R$  is calculated by taking into account the length of end windings  $L_{ew}$ :

$$R = \frac{2 N \rho_{copper} (L + L_{ew})}{S_c} \quad (11)$$

Where  $S_c$  is the conductor cross-section. The end winding length is calculated in the middle of the slot from this equation:

$$L_{ew} = \frac{(w_d + \frac{\pi \tau_s}{2})}{2} \quad (12)$$

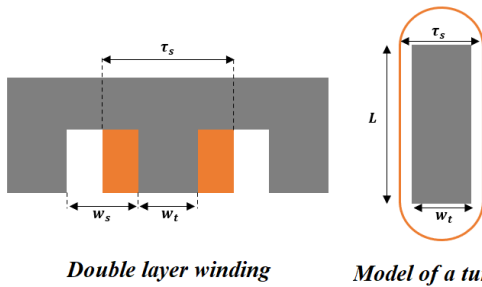


Fig. 2. Representation of a double layer winding and corresponding end windings.

According to the output power and losses of PMSM, the efficiency  $\eta$  can be determined as follows:

$$\eta = \frac{\omega_r T}{\omega_r T + P_{Joule} + P_{iron}} \quad (13)$$

#### F. Calculation of Motor Volumes and Masses

The motor masses are obtained from the volume of each constitutive element and from the corresponding mass densities  $\rho$ .

The magnet volume  $V_{magnet}$  can be approximated as:

$$V_{magnet} = 4 p h_{pm} e_{pm} L \quad (14)$$

where  $p$  is the pole pair,  $h_{pm}$  the magnet width and  $e_{pm}$  the magnet thickness.

The magnet mass  $M_{magnet}$  is given by:

$$M_{magnet} = \rho_{magnet} V_{magnet} \quad (15)$$

The copper volume and mass can be approximated by:

$$V_{copper} = 6 N (L + L_{ew}) S_c \quad (16)$$

$$M_{copper} = \rho_{copper} V_{copper} \quad (17)$$

The stator volume  $V_{stator}$  is composed of yoke and teeth volumes

$$V_{stator} = V_{yoke} + V_{teeth} \quad (18)$$

They can be approximated by:

$$\begin{cases} V_{yoke} = \pi (R_o^2 - (R_s + h_s)^2) L \\ V_{teeth} \approx Q_s \left( w_t (h_s - h_t) + \frac{w_t + (\tau_s - o_s)}{2} \right) L \end{cases} \quad (19)$$

where  $R_o$  is the outer radius of the stator,  $R_s$  the inner radius of the stator,  $Q_s$  the slot number,  $h_s$  the slot depth,  $w_t$  the tooth width,  $\tau_s$  the slot pitch, and  $o_s$  the slot opening.

The corresponding mass is calculated as:

$$M_{stator} \approx \rho_{iron} V_{stator} \quad (20)$$

The rotor volume and mass can be approximated by (12) and (13) where  $R_i$  is the inner radius of rotor:

$$V_{rotor} = \pi (R_r^2 - R_i^2) L - V_{magnet} \quad (21)$$

$$M_{rotor} = \rho_{iron} V_{rotor} \quad (22)$$

### III. FORMULATION OF THE OPTIMIZATION PROBLEM

In order to increase the power density and the efficiency at the same time, the best trade-off solution must be found. A multi-objective algorithm is used. In [14], the authors proposed a new version of the NSGA algorithm, NSGA2 (Non-Dominated Genetic Sorting Algorithm), which is more efficient than its predecessor. The different steps of the optimization are shown in Fig.3.

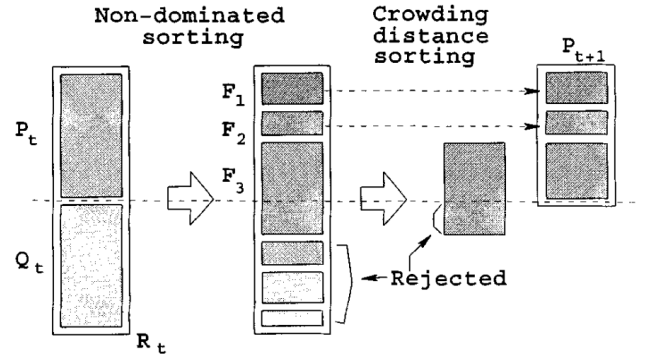


Fig. 3. Representation of the different optimization steps by NSGA2 [14].

The different steps of NSGA2 optimization are [14]:

- Step 1: An initial population is randomly generated;
- Step 2: Objective functions are evaluated for each individual in the population and thus the best individuals are selected by elitism;
- Step 3: The unselected individuals will undergo crossover and mutation to form a new population, which will be subjected to the previous steps again. The process continues, from one generation to the next, until a stop criterion is reached.

In this study, the optimization criteria are the power density and the efficiency of the machine. Tables 2, 3, and 4 give respectively the optimization parameters and their range, the optimization constraints referred to the bibliography [13] [15] [16], and the optimization tool parameters of NSGA2. All optimization parameters are of continuous type.

TABLE 2  
DOMAIN OF VARIATION OF THE OPTIMIZATION PARAMETERS

Parameters	Range
Magnet width (mm)	[1, 10]
Magnet length (mm)	[10, 50]
Current density (A/mm <sup>2</sup> )	[1, 30]
Inner radius of stator (mm)	[70, 90]
Axial length (mm)	[70, 140]
Width teeth (mm)	[10-25]
Stator yoke (mm)	[1-20]

TABLE 3  
THE OPTIMIZATION CONSTRAINTS

Optimization Constraints	Min Value	Max Value
Airgap flux density (T)	0.8	-
Stator yoke flux density (T)	-	1.6
Stator tooth flux density (T)	-	1.8
Induced voltage (V)	-	$\frac{U_{DC}}{\sqrt{3}}$
peripheral speed (m/s)	-	130
Slot depth (mm)	-	4 × Slot depth

TABLE 4  
OPTIMIZATION TOOL PARAMETERS

Parameters	Values
Number of individuals	100
Number of generations	200
Number of variables	7
Number of constraints	5
Number of criteria	2

#### IV. RESULTS OF THE OPTIMIZATION

The previously described genetic algorithm has been applied to maximize the power density and efficiency of the 12/8 topology. This topology, quite classical in the literature, is a good test case for our algorithm. Based on the previously defined specifications, the objective functions (efficiency and power density) have been drawn as a function of the current density and are presented in figures 4, 5 and 6.

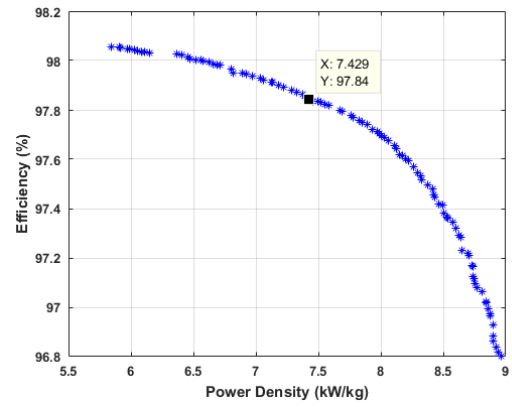


Fig. 4. Variation of the optimization criteria.

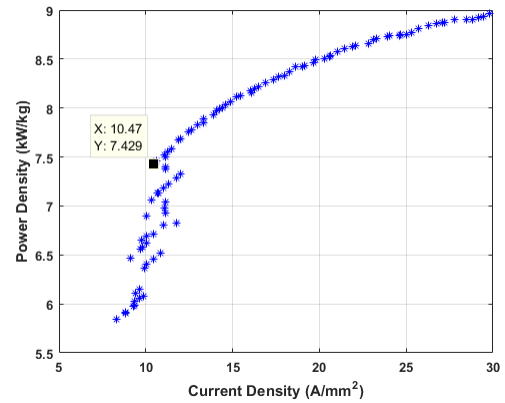


Fig. 5. Variation of the power density as a function of the current density.

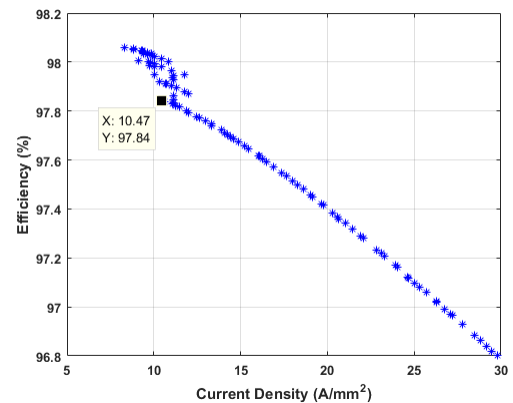


Fig. 6. Variation of the efficiency as a function of the current density.

The Fig. 4 shows that the efficiency decreases when the power density increases. Fig. 5 and 6 show that the increase of the current density leads to a decrease of the efficiency with an increase of the power density. The selected point highlighted on the curves are used in part five to validate the analytical design.

More parameters that greatly influence the power density can be identified. To do that, the variations of the objective functions for several operating points (different powers, different speeds, different voltage levels) are presented in Fig. 7, 8, and 9. In Fig. 7, the speed has been set to 10000 rpm and the DC voltage to 900V; optimization criteria can be shown for different mechanical power values (115, 145 and 175kW). The Fig. 8 shows the optimization criteria for mechanical power and DC voltage set to 115kW and 900V respectively and for different speed values (10000, 12500 and 15000rpm).

In figure 9, the mechanical power has been set to 115kW and the rotational speed to 10000 rpm; the optimization criteria are shown for different DC voltage values (400, 650 and 900V). The Fig. 7 shows clearly that the mechanical power increase leads to variations of efficiency and power density. However, increasing the rotational speed increases the power density but decreases the efficiency of the machine (Fig.8). This can be explained by the increase in iron losses. The increase in voltage “only” causes a very slight decrease in power density and efficiency (Fig.9), which is due to the increase in the number of turns.

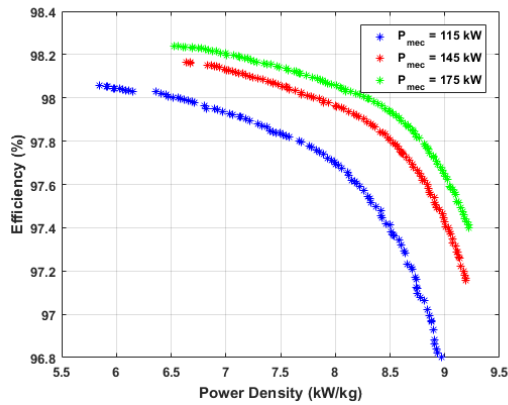


Fig. 7. Variation of the optimization criteria for different mechanical powers.

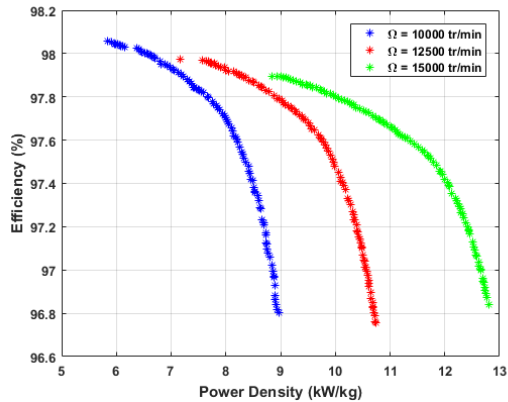


Fig. 8. Variation of the optimization criteria for different rotational speeds.

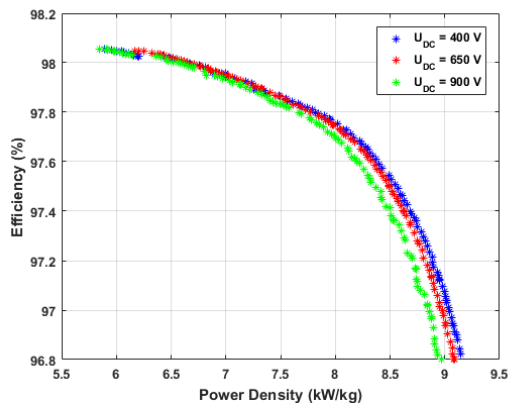


Fig. 9. Variation of the optimization criteria for different DC voltages.

## V. FINITE ELEMENT SIMULATION

A good way to validate the analytical magnetic design is to perform FE simulations. The operating point defined from the design in part four is shown in table 5. The mesh geometry of this machine is given in Fig. 10.

The solution obtained by the analytical design is modelled using FLUX2D software and it allows to obtain the variation of the torque, as shown in Fig. 11. The relative error on the average torque between analytical and FE simulations results is about 4.33%. It confirms the reliability of the analytical design. In Fig. 12, the authors present the map of the magnetic flux density distribution in the magnetic circuit. It shows a local saturation in the rotor and in the tooth tips. In the teeth, the maximum magnetic flux density level is about 1.8 T. This value represents the saturation level of the NO20 electrical steel, which means that, magnetically, the teeth are fully exploited.

TABLE 5  
MOTOR PARAMETERS

Quantity	Value
DC voltage	900 V
Current	130 A
Stator inner radius	76 mm
Air gap length	1 mm
Yoke height	13.2 mm
Slot body width	20,1 mm
Slot opening	4,03 mm
Slot depth	15,56 mm
Stack length	80 mm
Magnet width	5,5 mm
Magnet length	24 mm
No of series turns per phase	36

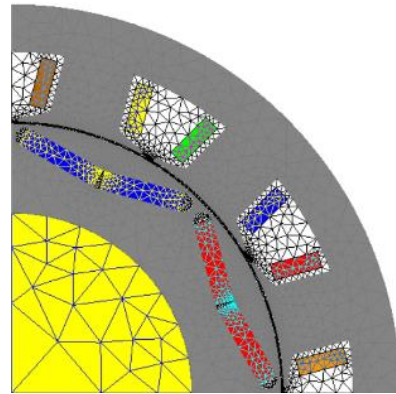


Fig. 10. Mesh of the studied IPM machine.

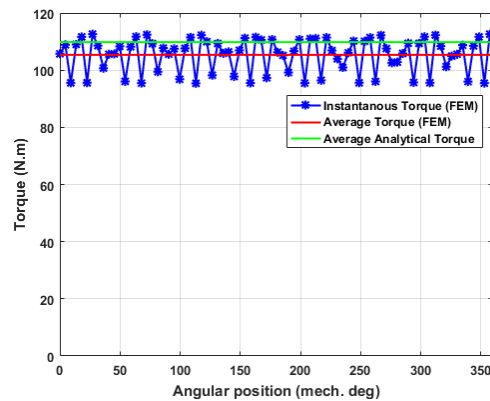


Fig. 11. Torque as function of angular position.

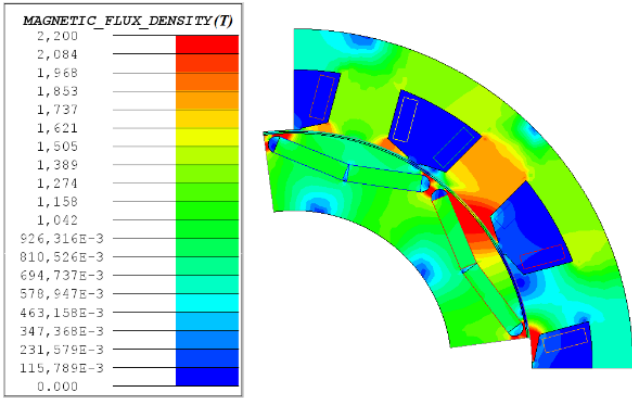


Fig. 12. Rated magnetic flux density.

The cycle efficiency for different operating points has been calculated as a function of load and speed. The efficiency map shown in Fig. 13 is plotted for both operating modes: constant torque and flux weakening. The map is calculated by FEM considering the iron losses, eddy current losses in the magnets and Joule losses considering coil -ends. The skin effect/proximity effect and the mechanical losses are not considered.

The energy efficiency is low at low speed and high torque. This is logical because the frequency is low and the Joule losses are high. It degrades with the flux-weakening as the speed increases and at low load.

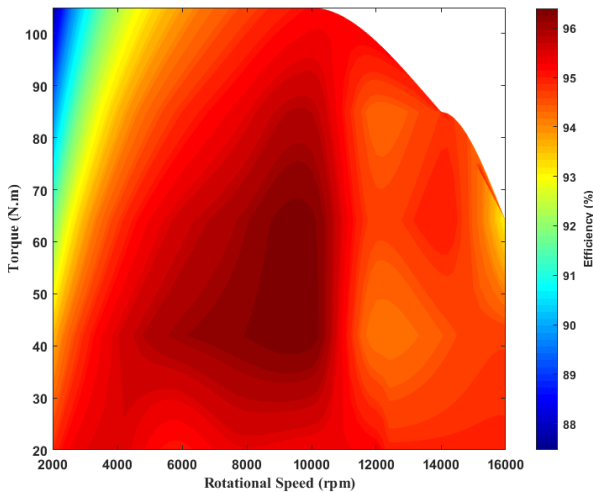


Fig. 13. Efficiency maps of the IPM motor.

## VI. CONCLUSION

In this paper, the authors proposed a method to maximize the power density of PMSM. The optimal design is based on a simplified analytical model combined with a genetic algorithm. The analytical magnetic sizing has been validated by FEM results, with a difference lower than 5%. If the power density can be increased by acting on the current density and the rotational speed, it is constrained by the thermal effect and by the mechanical effects. We can further increase the power density by changing the magnetic materials such as permanent magnets and steel sheets. As a perspective, using Grain Oriented Electrical Steel (GOES) or Cobalt Iron alloys (FeCo) as magnetic materials may be considered to improve the efficiency and power density.

## VII. ACKNOWLEDGMENT

This work is cofinanced by the French Region of Hauts-de-France and the urban community CABBALR (Communauté d'Agglomérations Béthune Bruay Artois Lys Romane). It is also coupled with a project entitled RedHAT (Reliable electrical machines with very hHigh tTorque and pPower densities) funded by the French National Research Agency (ANR).

## VIII. REFERENCES

- [1] R. Kobler, D. Andessner, G. Weidenholzer, and W. Amrhein, "Development of a compact and low cost axial flux machine using soft magnetic composite and hard ferrite," in Proceedings of the International Conference on Power Electronics and Drive Systems, Aug. 2015, vol. 2015-August, pp. 810–815.
- [2] R. Benlamine, T. Hamiti, F. Vangraefschep, and D. Lhotellier, "Electromagnetic, mechanical and thermal analysis of a high-speed surface-mounted PM machine for automotive application," in 2016 XXII International Conference on Electrical Machines (ICEM), Sep. 2016, pp. 1662–1667.
- [3] D. Son, D.-H. Lee, and J.-W. Ahn, "Design and analysis of double stator axial field type srm," in 2017 IEEE Transportation Electrification Conference and Expo, Asia-Pacific (ITEC Asia-Pacific), Aug. 2017, pp. 1–6.
- [4] Jurkovic, S., Rahman, K. M., Morgante, J. C., & Savagian, P. J. (2015). Induction Machine Design and Analysis for General Motors e-Assist Electrification Technology. IEEE Transactions on Industry Applications, 51(1), 631–639.
- [5] Z. Q. Zhu and D. Howe, "Electrical Machines and Drives for Electric, Hybrid, and Fuel Cell Vehicles," Proceedings of the IEEE, vol. 95, no. 4, pp. 746–765, Apr. 2007.
- [6] C. C. Chan, "The state of the art of electric and hybrid vehicles," Proceedings of the IEEE, vol. 90, no. 2, pp. 247–275, 2002.
- [7] A. Laidoudi, S. Duchesne, F. Morganti, and G. Velu, "High-power density induction machines with increased windings temperature," Open Physics, vol. 18, no. 1, pp. 642–651, Oct. 2020.
- [8] A. S. Nagorny, N. V. Dravid, R. H. Jansen, and B. H. Kenny, "Design aspects of a high speed permanent magnet synchronous motor / generator for flywheel applications," in IEEE International Conference on Electric Machines and Drives, 2005, pp. 635–641.
- [9] D. Kowal, P. Sergeant, L. Dupre, and A. van den Bossche, "Comparison of Nonoriented and Grain-Oriented Material in an Axial Flux Permanent-Magnet Machine," IEEE Transactions on Magnetics, vol. 46, no. 2, pp. 279–285, Feb. 2010.
- [10] J. Cros and P. Viarouge, "Synthesis of high performance PM motors with concentrated windings," IEEE Transactions on Energy Conversion, vol. 17, no. 2, pp. 248–253, Jun. 2002.
- [11] N. Bekka, M. E. H. Zaim, N. Bernard, and D. Trichet, "A Novel Methodology for Optimal Design of Fractional Slot With Concentrated Windings," IEEE Transactions on Energy Conversion, vol. 31, no. 3, pp. 1153–1160, Sep. 2016.
- [12] M. Farshadnia, Advanced Theory of Fractional-Slot Concentrated-Wound Permanent Magnet Synchronous Machines. Singapore: Springer Singapore, 2018.
- [13] J. Pyrhönen, T. Jokinen, and V. Hrabovcová, Design of Rotating Electrical Machines. Chichester, UK: John Wiley & Sons Ltd, 2013.
- [14] K. Deb, A. Pratap, S. Agarwal, and T. Meyarivan, "A fast and elitist multiobjective genetic algorithm: NSGA-II," IEEE Transactions on Evolutionary Computation, vol. 6, no. 2, pp. 182–197, Apr. 2002.
- [15] Rezzoug, Abderrezak., & el Hadi Zaïm, Mohamed. (2012). *Non-conventional electrical machines*. ISTE.
- [16] Borisavljevic, A. (2013). Limits, Modeling and Design of High-Speed Permanent Magnet Machines. Springer Berlin Heidelberg.

## IX. BIOGRAPHIES

**Mohamed Amine HEBRI** was born in Algiers, Algeria, in 1997. He received the Engineer Diploma degree and the MSc degree in Electrical Engineering from Ecole Nationale Polytechnique (ENP), Algiers, in 2020. In 2020, he joined Laboratoire Systèmes Electrotechniques et Environnement (LSEE), Artois University, France, as a Ph.D. Student. His research interests include electrical machine design, optimization, modeling, and simulation.

**Abderrahmane REBHAOUI** was born in Algiers, Algeria, in 1994. He received the Engineer Diploma degree in Electrical Engineering from Ecole Nationale Polytechnique (ENP), Algiers, in 2018. He received the MSc degree from the University of Le Havre Normandie, France, in 2019. He joined Institut VEDECOM, Versailles – France, in 2019, as a Ph.D. Student, in collaboration with Laboratoire Systèmes Electrotechniques et Environnement (LSEE), Artois University, France. His research work focuses on electric motor design, magnetic material characterisation and optimisation.

**Grégory Bauw** was born in France in 1992. He received the Master's degree of Electrical Engineering from Artois University, Béthune, France, in 2015, and the PhD degree from Artois University in 2018. He is currently associate professor with the LSEE (Laboratoire Systèmes Electrotechnique et Environnement), Artois University, France. His research interests include: noise and vibrations of electrical machines, reliability and aging of the electrical insulation system.

**Jean-Philippe Lecoïnte**, DSc, received the MSc degree in Electrical Engineering from the Université des Sciences et Technologies de Lille, France, in 2000. He received the PhD degree from the Université d'Artois, France, in 2003. He is currently Full Professor at the Artois University and he is the head of the LSEE (Electrical Systems and Environment Research Laboratory), France. His research interests focus on efficiency, noise and vibrations of electrical machines.

**Stephane Duchesne** was born in the north of France in 1977, he obtained his Master of Science from the University of Lille in 2000 and his Ph.D. in 2004 at the Artois University. He has been a full professor at the electrical engineering department of Artois University (LSEE - Laboratoire Systèmes Electrotechnique et environnement) since 2015. His research topics concern electrical machines operating in harsh operating conditions. He focuses especially on the electrical insulation system and its mechanisms of failure, its aging, and the evaluation of its health status.

**Vincent Mallard** received the master's degree in mechatronics engineering from the University of Technology of Compiègne, Compiègne, France, in 2013, and the Ph.D. degree in electrical engineering from the Artois University, Arras, France, in 2018. His research interests are in electric machines and drives, with focus on industrial and automotive applications. He is currently working on drives and power electronics with CRITT M2A, Bruay-la-Buissière, France.

**Gianluca Zito** received a Ph.D. degree in Automatic Control from the Grenoble Institute of Technology (Grenoble INP), France. He has 17 years of experience in innovative powertrain control. He has been involved in several research projects on energy management, transmission control of hybrid electric vehicles, advanced engine control and electric motor control (IPM, SPM and SynRel motors). He is currently working at IFP Energies nouvelles as project manager in innovative electric powertrain development.

**Abdenour Abdelli** was born in Azazga, Algeria, in 1977. He received the diploma of engineering degree in electrical engineering from the National Polytechnic School of Algiers, El-Harrach, Algeria, in 2003, and the Ph.D. degree in electrical engineering from the National Polytechnic Institute of Toulouse, Toulouse, France, in 2007. He joined IFP Energies Nouvelles in December 2008 as a Research Engineer. He is working on the research and the development of hybrid and electric vehicles. His research interests include the design and the modeling of electrical machines for hybrid and electric vehicles thanks to efficient numerical methods.

**Adrien Maier** was born in the north of France in 1998, he received the Technical University degree about Electrical Engineering in 2019, he keeps studying in the ESIEE engineering school with work-study contract about Electrical Engineering and Sustainable Development. As an apprentice in work-study contract, he is currently working at EREM in charge of project development.